

Experimental Section

Materials

MnSO₄ (≥99.0%), KMnO₄ (≥99.3%), Na₂SO₄ (≥99.0%), NaNO₃ (≥99.0%), C₇H₆O₃ (≥99.5%), KNaC₄H₁₂O₁₀·4H₂O (≥99.9%), NaOH (≥96%), NaClO (≥99.9 wt %), NaNO₂ (≥99.0%), NH₄Cl (≥99.5%), C₁₂H₁₄N₂·2HCl (≥99.0%), C₆H₈N₂O₂S (≥99.5%) were provided from Sigma-Aldrich Chemical Reagent Co., Ltd. and Sinopharm Chemical Reagent Co., Ltd. All of the reagents were of analytical grade and were used as received without further purification.

Synthesis of MnO₂ and MnO_{2-x} nanosheets

All reagents were directly used without further purification. The MnO₂ was prepared by a hydrothermal method. In brief, 70 mg MnSO₄ and 400 mg KMnO₄ were dissolved in 60 mL deionized water and stirred for 15 min. The mixed solution was transferred into a 100 mL Teflon-lined stainless-steel autoclave and maintained at 180 °C for 24 h. After the autoclave cooled down to room temperature, the MnO₂ was collected by centrifugation and washed with deionized water and absolute alcohol several times. To prepare MnO_{2-x}, the obtained MnO₂ was annealed at 500 °C for 2 h with heating rate of 2 °C min⁻¹ in Ar flow.

Electrochemical measurements

Electrochemical measurements are carried out on a CHI-660E electrochemical workstation using an H-type two-compartment electrochemical cell which was separated by a Nafion 211 membrane. The carbon cloth (CC) coated with catalyst, Hg/HgO and platinum foil were used as working, reference and counter electrode, respectively. The CC was immersed in 0.5 M H₂SO₄ for 12 h, and then washed with deionized water several times and dried at 60 °C for 24 h. For the working electrode, the catalyst inks were deposited onto the pretreated CC (1×1 cm², 0.2 mg cm⁻²) and dried in the air. Electrochemical NO₃RR tests were conducted in 0.1 M Na₂SO₄ with 0.1 M NaNO₃. The each chronoamperometric test was conducted for 2 h. All potentials were referenced to the reversible hydrogen electrode RHE ($E_{\text{RHE}} = E_{\text{Hg/HgO}}$

+ (0.098 + 0.0591 × pH).

Determination of NH₃

The concentration of produced NH₃ in neutral electrolyte were determined by the indophenol blue method¹. The 2 mL diluted electrolyte was moved into the mixed solution contained 2 mL 1 M NaOH solution, 5% salicylic acid and 5% potassium sodium tartrate tetrahydrate. Then, 1 mL 0.05 M NaClO and 0.2 mL Na₂Fe(CN)₅NO·2H₂O (1wt%) solution was moved into the prepared solution. The UV-vis absorption spectra were determined after standing for 2 h. Of note, taking the absorbance value of 655 nm served as the absorbance value for subsequent determination of NH₃. A series of NH₄Cl solutions with different concentrations were used to determine the standard curve to calculate the yields and FEs.

Calculation of NH₃ yield and Faradaic efficiency

$$\text{NH}_3 \text{ yield } (\mu\text{g h}^{-1} \text{ mg}_{\text{cat}}^{-1}) = \frac{c_{\text{NH}_3} \times V}{t \times m} \quad (1)$$

$$\text{Faradaic efficiency } (\%) = \frac{n \times F \times c_{\text{NH}_3} \times V}{M \times Q} \times 100\% \quad (2)$$

where n is the number of electrons transferred, F (96500 C mol⁻¹) is the Faraday constant, c_{NH_3} (μg mL⁻¹) is the measured NH₃ concentration, V (mL) is the volume of cathodic reaction electrolyte, M is the relative molecular mass of products, m is the amount of catalyst supported, Q (C) is the total quantity of applied electricity, t (h) is the reduction time, and A is the geometric area of working electrode.

Determination of NO₂⁻

The Griess test can be used to identify the concentration NO₂⁻ remaining in the reaction electrolyte. First, the Griess reagents were prepared by adding 0.1 g N-(1-naphthyl)-ethylenediamine dihydrochloride, 1.0 g sulfonamide and 2.94 mL H₃PO₄ in 50 mL deionized water. 0.5 mL electrolyte was diluted 50 times by adding deionized water, and then 0.1 mL chromogenic agent was added. After standing for 10 min, the absorbance curve was measured. In the wavelength range of 400-700 nm, take the absorbance value of 540 nm. A series of NaNO₂ solutions with different

concentrations were used to determine the standard curve, which was used to calculate NO_2^- yields and FEs.

Determination of N_2H_4

The 330 mL of color reagent were prepared by 300 mL of ethyl alcohol, 5.99 g of $\text{C}_9\text{H}_{11}\text{NO}$ and 30 mL of HCl , and 5 mL of color reagent was added into 5 mL of electrolyte. The UV-vis absorption spectrum was measured and took the absorbance value of 455 nm. The corresponding standard curves were calibrated by the standard N_2H_4 solution with a series of concentrations after stirring for 10 min.

Characterizations

X-ray diffraction (XRD) pattern was collected on a Rigaku D/max 2400 diffractometer. Transmission electron microscopy (TEM) and high-resolution transmission electron microscopy (HRTEM) images were carried out on a Tecnai G² F20 microscope. X-ray photoelectron spectroscopy (XPS) analysis was conducted on a PHI 5702 spectrometer. ^1H nuclear magnetic resonance (NMR) measurements were conducted on a 500 MHz Bruker superconducting-magnet NMR spectrometer. Electron paramagnetic resonance (EPR) measurements were performed on a Bruker ESP-300 spectrometer.

Calculation details

DFT calculations were conducted using a Cambridge sequential total energy package (CASTEP). The generalized gradient approximation (GGA) with Perdew-Burke-Ernzerhof (PBE) functional was used to model the exchange-correlation interactions. The van der Waals (vdW) interaction was calculated based on a DFT-D method. The electron wave functions were expanded by plane waves with a cutoff energy of 400 eV, and a Monkhorst-Pack grid ($3 \times 3 \times 1$) was used for k-point sampling. The convergence of energy and forces were set to be 2×10^{-5} eV and 0.01 eV \AA^{-1} , respectively. MnO_2 (001) slab was modeled by a $4 \times 4 \times 1$ supercell, and a vacuum space of around 15 \AA was set along the z direction to avoid the interaction between periodical images.

The adsorption energy (ΔE) is defined as²

$$\Delta E = E_{\text{ads/slab}} - E_{\text{ads}} - E_{\text{slab}} \quad (3)$$

where $E_{\text{ads/slab}}$, E_{ads} and E_{slab} are the total energies for adsorbed species on slab, adsorbed species and isolated slab, respectively.

The Gibbs free energy (ΔG , 298.15 K) of reaction steps is calculated by:

$$\Delta G = \Delta E + \Delta ZPE - T\Delta S \quad (4)$$

where ΔE is the adsorption energy, ΔZPE is the zero-point energy difference and $T\Delta S$ is the entropy difference between the gas phase and adsorbed state. The entropies of free gases were acquired from the NIST database.

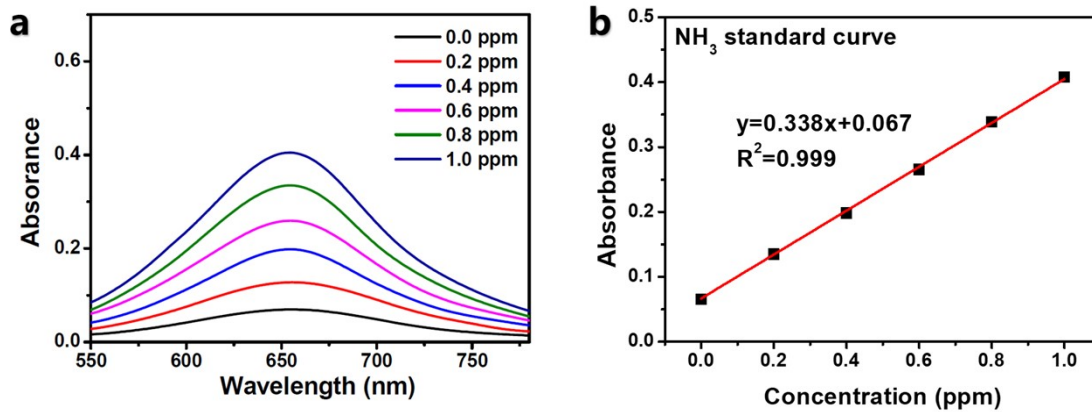


Fig. S1. (a) UV-vis absorption spectra and (b) corresponding calibration curve used for calculation of NH_3 concentration.

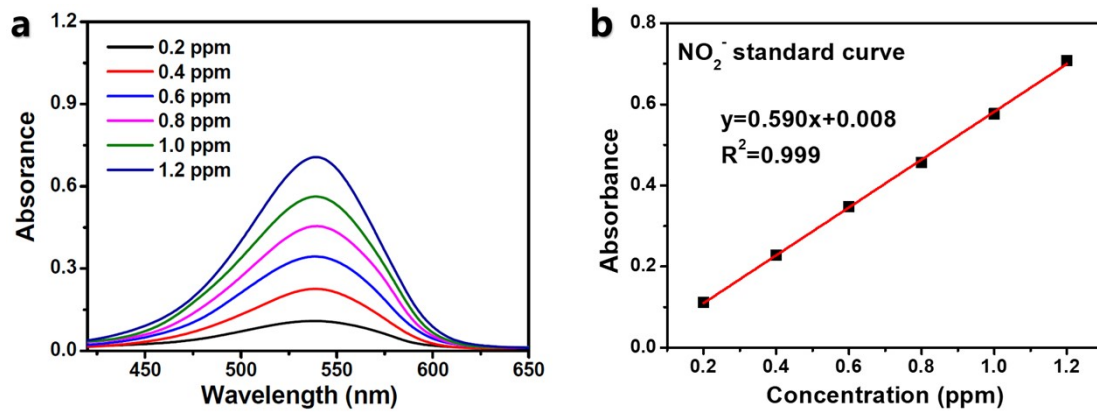


Fig. S2. (a) UV-vis absorption spectra and (b) corresponding calibration curve used for calculation of NO_2^- concentration.

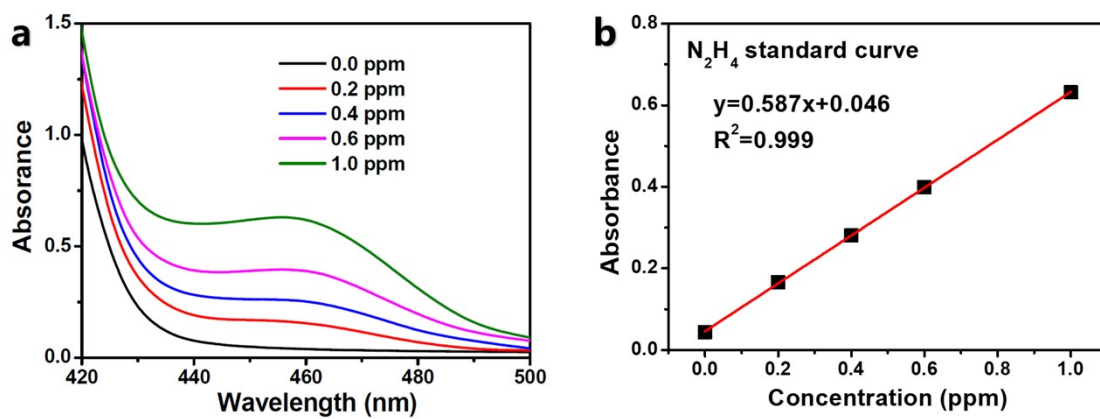


Fig. S3. (a) UV-vis absorption spectra and (b) corresponding calibration curve used for calculation of N_2H_4 concentration.

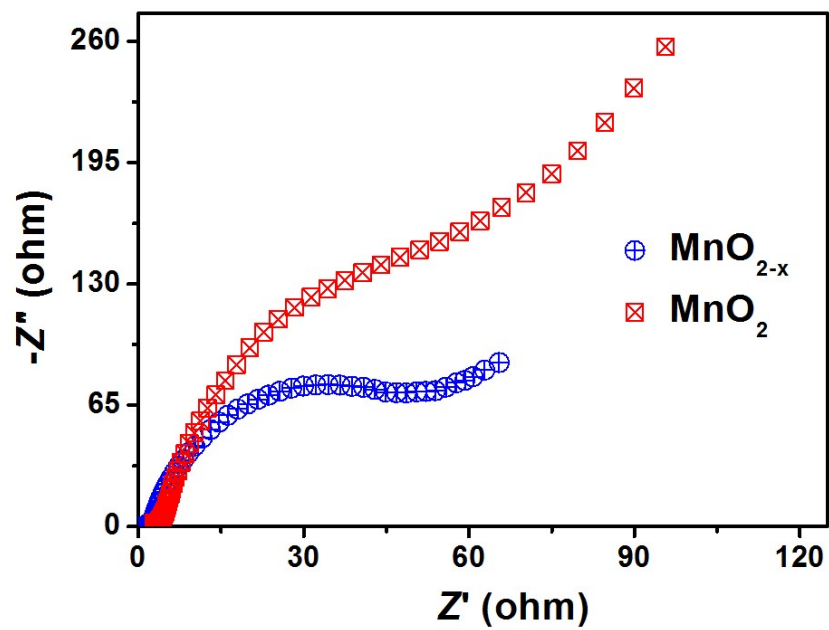


Fig. S4. Electrochemical impedance spectra of MnO_{2-x} and MnO_2 .

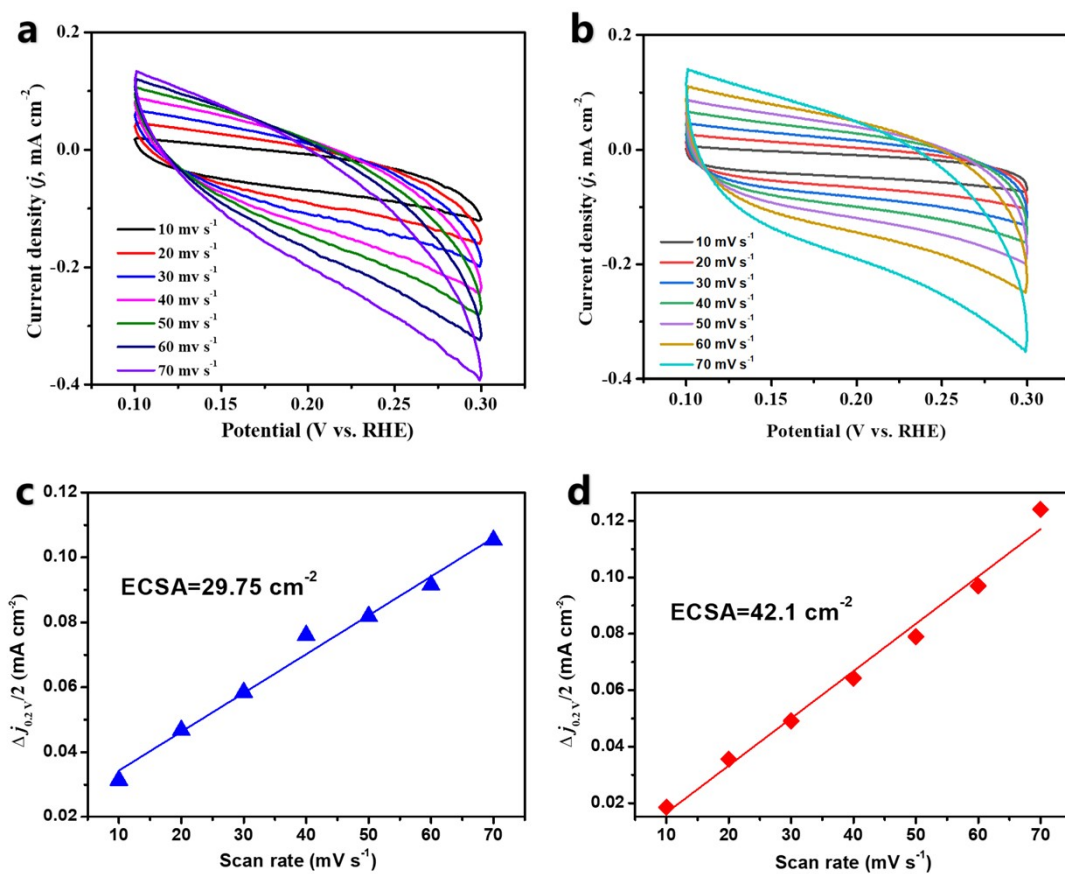


Fig. S5. Electrochemical double-layer capacitance (C_{dl}) measurements at different scanning rates of 10~70 mV s⁻¹ for (a, c) MnO₂ and (b, d) MnO_{2-x}.

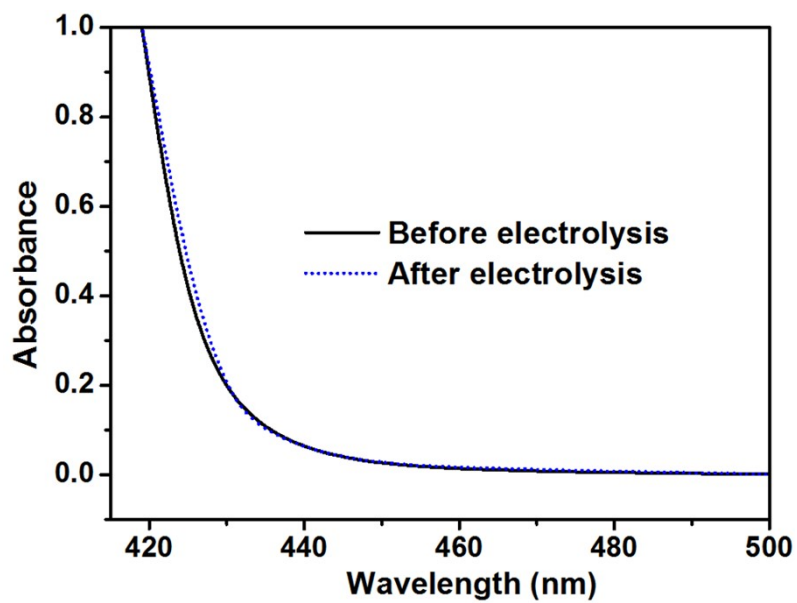


Fig. S6. UV-vis spectra of the electrolytes before and after 2 h electrocatalysis on MnO_{2-x} at -0.9 V.

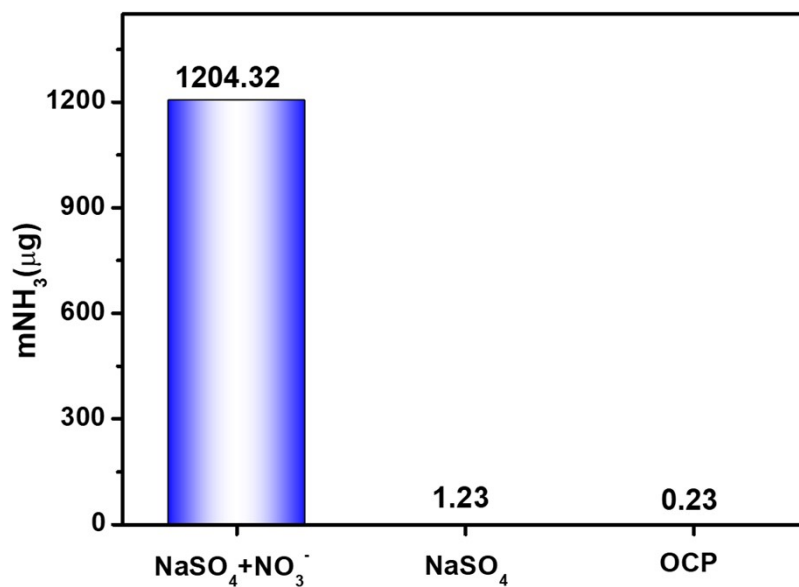


Fig. S7. Amounts of produced NH₃ under different operating conditions of NO₃RR.

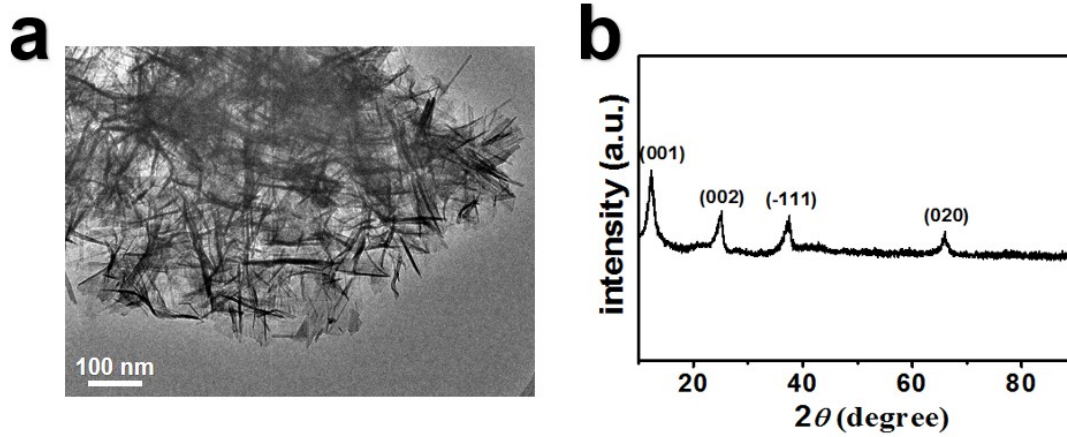


Fig. S8. (a) TEM images and (b) XRD pattern of MnO_{2-x} after stability tests.

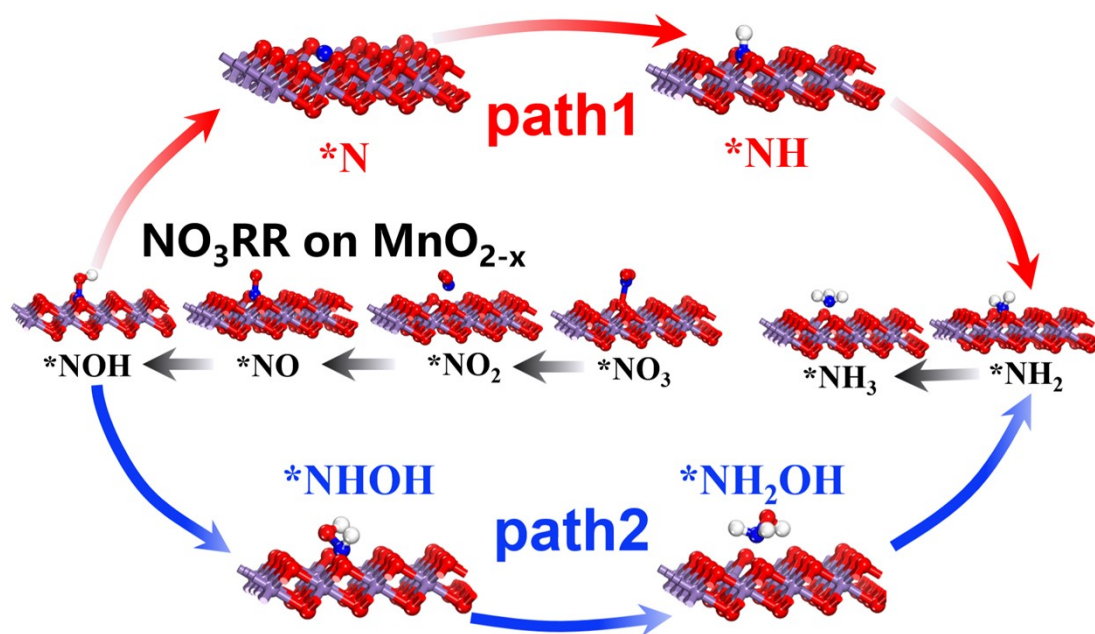


Fig. S9. Optimized structures of NO₃RR intermediates on MnO_{2-x}.

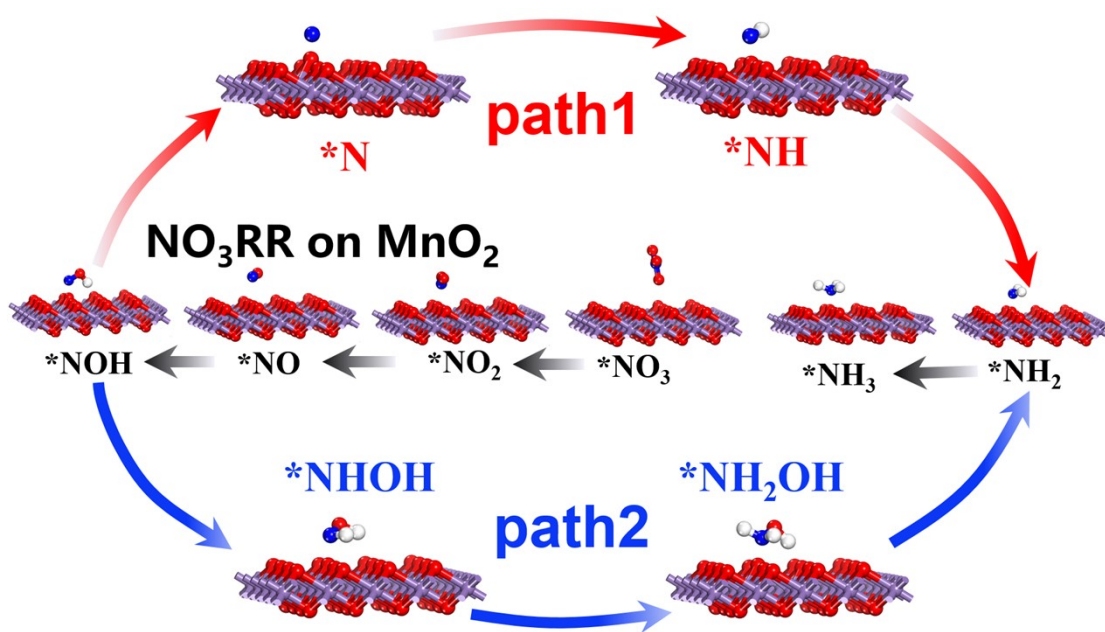


Fig. S10. Optimized structures of NO₃RR intermediates on MnO₂.

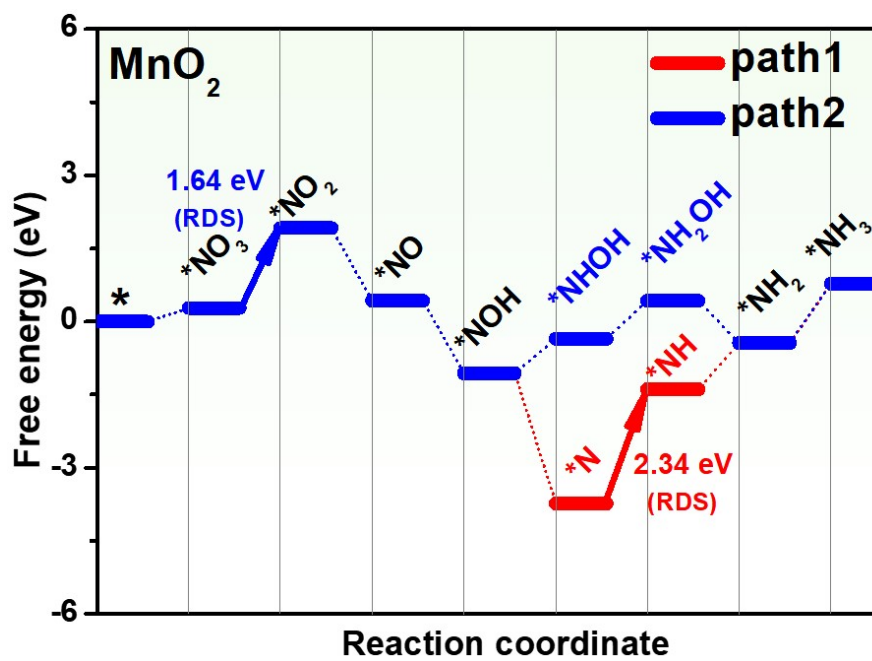


Fig. S11. Gibbs free energy diagram of NO₃RR pathway on MnO₂.

Table S1. Comparison of NH₃ yield and Faradic efficiency for recently reported NO₃RR electrocatalysts at ambient conditions

Catalyst	Electrolyte	NH ₃ yield rate & Optimum Potential (mg h ⁻¹ cm ⁻²)	FE & Optimum Potential (V vs RHE)	Ref.
Co ₂ AlO ₄ /CC	0.1 M PBS (0.1 M NO ₃ ⁻)	7.9@-0.7	92.6%@-0.7	3
Cu-PTCDA	1 M PBS (500 ppm KNO ₃)	0.436 @-0.4	85.9%@-0.4	4
Pd/TiO ₂	1 M LiCl (0.25 M K ¹⁵ NO ₃)	1.12@-0.8	92.1%@-0.7	5
CuCl_BEF	0.5 M Na ₂ SO ₄ (100 mg/LNO ₃ ⁻)	1.82@-1.0	44.7%@-1.0	6
CoP NWAs	1 M NaOH (0.5 mM NaNO ₃)	0.317@-0.7	65%@-0.4	7
Nix/NC-sd	0.5 M Na ₂ SO ₄ (0.3M NO ₃ ⁻)	25.1@-0.5	99%@-0.5	8
Poly-Cu ₁₄ cba	0.5 M K ₂ SO ₄ (250 ppm NO ₃ ⁻)	2.848@-1.05	90%@-1.05	9
CuO NWAs	0.5 M Na ₂ SO ₄ (200 ppm NO ₃ ⁻)	4.163@-0.85	95.8%@-0.85	10
CF@Cu ₂ O	0.1 M PBS (0.1 M NaNO ₂)	7.511@-0.6	94.21%@-0.6	11
Pd facets	1 M NaOH (20 mM NO ₃ ⁻)	0.3068@-0.2	35%@-0.2	12
MnO_{2-x}	0.5 M Na₂SO₄ (0.1 M NO₃⁻)	3.34@-1.0	92.4%@-0.9	This work

Supplementary references

1. J. R. Christianson, D. Zhu, R. J. Hamers and J. R. Schmidt, *J. Phys. Chem. B*, 2013, **118**, 195-203.
2. A. A. Peterson, *Energy Environ. Sci.*, 2010, **3**, 1311-1315.
3. Z. Deng, J. Liang, Q. Liu, C. Ma, L. Xie, L. Yue, Y. Ren, T. Li, Y. Luo, N. Li, B. Tang, A. Ali Alshehri, I. Shakir, P. O. Agboola, S. Yan, B. Zheng, J. Du, Q. Kong and X. Sun, *Chem. Eng. J.*, 2022, **435**, 135104.
4. G.-F. Chen, Y. Yuan, H. Jiang, S.-Y. Ren, L.-X. Ding, L. Ma, T. Wu, J. Lu and H. Wang, *Nat. Energy*, 2020, **5**, 605-613.
5. Y. Guo, R. Zhang, S. Zhang, Y. Zhao, Q. Yang, Z. Huang, B. Dong and C. Zhi, *Energy Environ. Sci.*, 2021, **14**, 3938-3944.
6. W. J. Sun, H. Q. Ji, L. X. Li, H. Y. Zhang, Z. K. Wang, J. H. He and J. M. Lu, *Angew. Chem. Int. Ed.*, 2021, **60**, 22933-22939.
7. H. Zhang, G. Wang, C. Wang, Y. Liu, Y. Yang, C. Wang, W. Jiang, L. Fu and J. Xu, *J. Electroanal. Chem.*, 2022, **910**, 116171.
8. P. Gao, Z. H. Xue, S. N. Zhang, D. Xu, G. Y. Zhai, Q. Y. Li, J. S. Chen and X. H. Li, *Angew. Chem. Int. Ed.*, 2021, **60**, 20711-20716.
9. Y. M. Wang, J. Cai, Q. Y. Wang, Y. Li, Z. Han, S. Li, C. H. Gong, S. Wang, S. Q. Zang and T. C. W. Mak, *Angew. Chem. Int. Ed.*, 2022, **61**, e202114538.
10. Y. Wang, W. Zhou, R. Jia, Y. Yu and B. Zhang, *Angew. Chem. Int. Ed.*, 2020, **59**, 5350-5354.
11. Q. Chen, X. An, Q. Liu, X. Wu, L. Xie, J. Zhang, W. Yao, M. S. Hamdy, Q. Kong and X. Sun, *Chem. Commun*, 2022, **58**, 517-520.
12. J. Lim, C.-Y. Liu, J. Park, Y.-H. Liu, T. P. Senftle, S. W. Lee and M. C. Hatzell, *ACS Catal.*, 2021, **11**, 7568-7577.